Review

Chinese Science Bulletin

SPECIAL TOPIC: Space Physics & Space Weather
Geophysics

April 2011 Vol.56 No.12: 1174–1181
doi: 10.1007/s11434-011-4440-0

Electron dynamics in collisionless magnetic reconnection

LU QuanMing[1], WANG RongSheng[2], XIE JinLin[3], HUANG Can[1], LU San[1] & WANG Shui[1]

[1] *CAS Key Laboratory of Basic Plasma Physics, School of Earth and Space Sciences, University of Science and Technology of China, Hefei 230026, China;*
[2] *Institute of Geology of Geophysics, Chinese Academy of Sciences, Beijing 100029, China;*
[3] *CAS Key Laboratory of Basic Plasma Physics, School of Physical Sciences, University of Science and Technology of China, Hefei 230026, China*

Received December 31, 2010; accepted January 21, 2011

Magnetic reconnection provides a physical mechanism for fast energy conversion from magnetic energy to plasma kinetic energy. It is closely associated with many explosive phenomena in space plasma, usually collisionless in character. For this reason, researchers have become more interested in collisionless magnetic reconnection. In this paper, the various roles of electron dynamics in collisionless magnetic reconnection are reviewed. First, at the ion inertial length scale, ions and electrons are decoupled. The resulting Hall effect determines the reconnection electric field. Moreover, electron motions determine the current system inside the reconnection plane and the electron density cavity along the separatrices. The current system in this plane produces an out-of-plane magnetic field. Second, at the electron inertial length scale, the anisotropy of electron pressure determines the magnitude of the reconnection electric field in this region. The production of energetic electrons, which is an important characteristic during magnetic reconnection, is accelerated by the reconnection electric field. In addition, the different topologies, temporal evolution and spatial distribution of the magnetic field affect the accelerating process of electrons and determine the final energy of the accelerated electrons. Third, we discuss results from simulations and spacecraft observations on the secondary magnetic islands produced due to secondary instabilities around the X point, and the associated energetic electrons. Furthermore, progress in laboratory plasma studies is also discussed in regard to electron dynamics during magnetic reconnection. Finally, some unresolved problems are presented.

magnetic reconnection, reconnection electric field, secondary island, electron acceleration

Citation: Lu Q M, Wang R S, Xie J L, et al. Electron dynamics in collisionless magnetic reconnection. Chinese Sci Bull, 2011, 56: 1174–1181, doi: 10.1007/s11434-011-4440-0

Magnetic reconnection provides an effective mechanism for fast conversion of magnetic energy into plasma kinetic energy. Simultaneously, the topology of magnetic field changes [1–3]. First proposed by Giovanelli, magnetic reconnection is related to many explosive phenomena, such as solar flares, magnetospheric substorms, and disruptive instabilities in Tokamak plasmas [4–8]. Giovanelli thought discharge phenomena would occur around the neutral line or point where the magnetic field vanishes, an idea that could be very important in solar-flare production [9]. In 1958, Dungey first introduced the concept of "magnetic reconnection" , applying it in the construction of the open Earth magnetosphere model [10]. The first magnetic reconnection model was proposed by Sweet and Parker, separately. In this model, plasma and magnetic field flow into the center of the current sheet from both sides where magnetic field lines are cut off and reconnected. Magnetic energy is converted into plasma kinetic energy; energized plasma then flows out of the region from both ends [11,12]. However, the predicted reconnection rate in this model is so low that it is unable to account for the explosive phenomena in space. Petschek improved the Sweet-Parker model and suggested that magnetic reconnection occurs in any system with two pairs of slow shock and X-line structure [13]. Although the reconnection rate in Petschek model is significantly larger than that in Sweet-Parker's, the rate is still too

*Corresponding author (email: qmlu@ustc.edu.cn)

slow to explain explosive phenomena in space plasma. Note, these earlier magnetic reconnection models are based on magnetohydrodynamics (MHD) equations in which energy is dissipated by resistance.

However, plasmas are usually very tenuous in space, the typical time scale over which a plasma parameter can change significantly is much smaller than the collision time scale of charged particles. Thus, plasmas are essentially collisionless in space and classical resistance is meaningless; in other words, magnetic reconnection in space is collisionless. Geospace Environmental Modeling (GEM) magnetic reconnection studies indicate that the Hall effect has a decisive role [14]. Using different simulation methods (MHD, Hall MHD, hybrid and particle-in-cell (PIC) simulations), 2-D magnetic reconnection under the same conditions has been explored. The results indicated that the reconnection rate is nearly the same in Hall MHD, hybrid and PIC simulations, and the reconnection region consists of a multiple scale structure. In scales larger than the ion inertial length, plasma is frozen-in along magnetic field lines and flows out of the current sheet with the Alfvén speed. Below the ion inertial length scale, electrons are still frozen-in along magnetic field lines but ions decouple from these lines. Thus, ions and electrons, moving differently, produce a Hall effect that determines the reconnection rate [14–21]. These different motions form a current system in the reconnection plane which creates an out-of-plane magnetic field. Moreover, the electron outflow can be characterized by velocities far larger than the Alfvén speed [15,22–25]. Below the electron inertial length scale, even electrons are no longer frozen-in along the magnetic field lines. The electron inertial term and anisotropic electron pressure term have important roles [18,26–31]. The reconnection rate is dominated by the Hall effect because of the electron inertial length being smaller than the ion inertial length.

Obviously, electron dynamics is very important in collisionless magnetic reconnection. First, electrons have a crucial role in forming the structure at the electron inertial length scale and determine the reconnection electric field in magnetic reconnection. Second, energetic electrons are an important characteristic, but how these energetic electrons are produced is also an outstanding issue. We also discuss below the secondary islands that arise from instabilities around X-line, and the relation between islands and energetic electrons. Finally, we summarize the progress of electron dynamics in laboratory magnetic reconnection.

1 Characteristics of the reconnection diffusion region

Inside the ion inertial region of collisionless magnetic reconnection, while ions are decoupled from the magnetic field lines, electrons are still frozen-in along these lines. The current in the reconnection plane is dominated by electron motion [32]. In anti-parallel magnetic reconnection, electrons stream along the separatrices from the strong magnetic field region into the X-line region where electrons are accelerated by the reconnection electric field. The accelerated electrons flow out along the magnetic field lines on the inside of the separatrices [21,32]. Thus, a current system is formed that streams out along the separatrices and flows into the X-line along these magnetic field lines inside the separatrices [23,32]. The out-of-plane magnetic field created by the current system will be cancelled, while a quadrupolar structure is formed inside the ion diffusion region [14,23,32]. The quadrupolar structure in the magnetotail associated with B_y has been demonstrated by the Wind satellite [22]. The low energy electron beam flowing into the X-line region is also detected in the boundary of the current sheet [22]. Not only these beams, but also the energetic electron beams streaming out of the X-line region were measured by the Cluster spacecraft [21,33–36]. These observations confirmed the theoretical results for the in-plane current system, i.e. the in-plane current jets flows out along the separatrices and into the X-line region inside the separatrices within the ion diffusion region [14,23,24]. Furthermore, the issue has been explored from another perspective. Lu et al. [32] found that while electrons are flowing into the X-line region, an electron density cavity is created. This cavity was first observed by the Wind, and then detected by the Cluster spacecraft [22,37–39]. The expectation, subsequently confirmed by Cluster, was that the maximum of B_y should appear in the middle of the current system, specifically closer to the center of the current sheet than the electron cavity, as shown in Figure 1(a). The observation indirectly verified the presence of the current system in the reconnection plane [32].

During magnetic reconnection with a guide field, the symmetric structures of the out-of-plane B_y and the electron density are altered as the guide field increases, and the reconnection rate decreases slowly. While the guide field is strong enough and comparable to the magnitude to the magnetic field out of the current sheet, the reconnection rate drops significantly [25,40]. Electrons stream into the X-point along one pair of separatrices, whereas along the other pair of separatrices, electrons stream out of the X-point. Thus the out-of-plane magnetic field B_y is enhanced in the center of the current sheet. The electron density cavity only appears in the separatrices along which electrons flow into the X-point [41], as shown in Figure 1(b).

The reconnection electric field, a quantity characterizing the reconnection rate, exists in the electron diffusion and magnetic pileup regions; the field center is situated at the X-point. According to the two-fluid model, the generalized Ohm's law can be deduced directly from the particle momentum equation [42],

$$\mathbf{E} = -\mathbf{V}_{\mathrm{i}} \times \mathbf{B} + \frac{1}{ne}\mathbf{j} \times \mathbf{B} - \frac{m_e}{e}\frac{\mathrm{d}\mathbf{V}_e}{\mathrm{d}t} - \frac{1}{ne}\nabla \cdot \ddot{P}^{(e)}. \qquad (1)$$

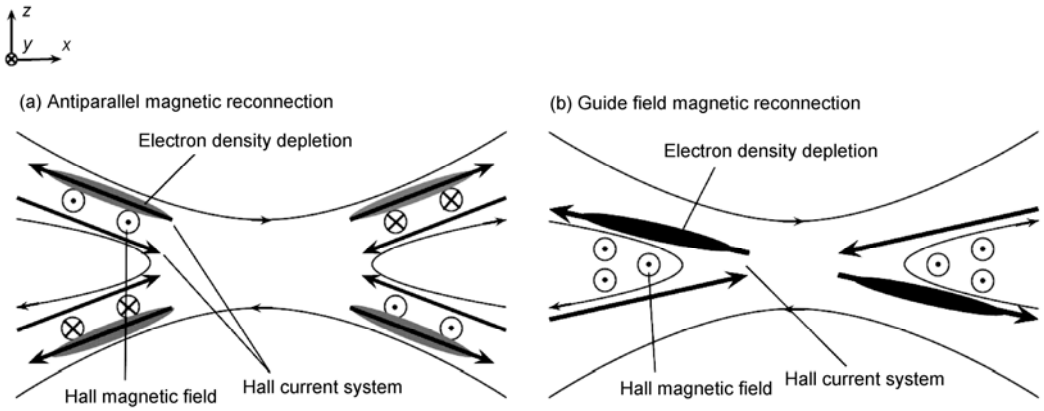

Figure 1 Hall current system, Hall magnetic field and electron density cavity in anti-parallel reconnection (a) and guide field reconnection (b).

The quasi-neutral assumption is used, i.e. $n_i \approx n_e \approx n$. Here V_i and V_e denote the average velocity of ions and electrons, respectively. The current density is defined as $\mathbf{j}=ne(V_i-V_e)$, and $\tilde{P}^{(e)}$ represents the electron pressure tensor. Assuming collisionless magnetic reconnection, the collision term is neglected in this generalized Ohm's law.

In the 2-D system ($\partial/\partial y = 0$), the y component of the generalized Ohm's law can be written in the form

$$\begin{aligned} E_y = &-(V_{iz}B_x - V_{ix}B_z) + \frac{1}{ne}(j_z B_x - j_x B_z) \\ &-\frac{m_e}{e}\left(\frac{\partial V_{ey}}{\partial t} + V_{ex}\frac{\partial V_{ey}}{\partial x} + V_{ez}\frac{\partial V_{ey}}{\partial z}\right) \\ &-\frac{1}{ne}\left(\frac{\partial P_{xy}^{(e)}}{\partial x} + \frac{\partial P_{zy}^{(e)}}{\partial z}\right). \end{aligned} \tag{2}$$

The first term is the Lorentz or convection term, the second term the Hall term, the third term the electron inertial term, and finally the electron pressure gradient term [18]. In anti-parallel magnetic reconnection, inside the electron inertial region, the convection and Hall terms in the generalized Ohm's law are negligible due to the weak magnetic field. Thus, the reconnection electric field inside the electron diffusion region mainly comes from the off-diagonal term of the electron pressure. In other words, the reconnection electric field is determined by an anisotropic electron pressure distribution [18,26]. Note that the off-diagonal term of this pressure tensor arises because of deviations from the Maxwell distribution [31]. Outside the electron diffusion region, especially around the pileup region, convection and Hall terms become larger than those in the electron diffusion region due to the strong z-component of the magnetic field. In this region, the reconnection electric field mainly comes from the convection and Hall terms, while the electron pressure gradient term and electron inertial term can be omitted. On further analysis, the distributions of the convective and Hall terms are different. The convection term is mainly distributed in the pileup region because ions can cross these magnetic field lines, which are primarily in-plane. The Hall term is mostly distributed inside the charge separation region, i.e. the separatrix region [18].

In magnetic reconnection with a guide field, the in-plane electric field and the magnetic field topology are similar to that in anti-parallel magnetic reconnection. As mentioned above, however, the reconnection rate will gradually diminish with the enhancement of the guide field. That is to say, the reconnection electric field weakens as the guide field increases [40]. Even with the presence of a guide field, the magnetic field strength inside the reconnection plane is still very low so that the reconnection electric field within the electron diffusion region is mainly produced by the electron pressure gradient term. Outside the electron diffusion region, the reconnection electric field stems mainly from the convection and Hall terms, similar to anti-parallel reconnection. Electron and ion flow velocities inside the reconnection plane are smaller than those found in anti-parallel reconnection because of the guide field. Again, the reconnection electric field will decrease because of the decrease of the convection and Hall terms. These terms also explain why the reconnection electric field diminishes as the guide field increases.

2 Electron acceleration within the reconnection diffusion region

Magnetic reconnection is an important mechanism for the production of energetic electrons that have been observed by *in situ* spacecraft [43–45]. Generally speaking, the reconnection electric field has a crucial role in accelerating electrons. Recently, significant progress has been achieved in full particle simulations. The results suggest that in anti-parallel reconnection electrons can be accelerated not only around the X-line region, but also in the pileup region of magnetic field [46]. Close to the X-line region, electrons with vanishing horizontal drift, $v_x \approx 0$, can be accelerated by the reconnection electric field to relativistic velocities [47].

These accelerated electrons gyrate along the magnetic field lines with velocities becoming diverted from the *y*-direction into the reconnection plane, and eventually flowing out of the X-point along the magnetic field lines [25,48]. In magnetic reconnection with an initial guide field, there is a very strong electric field parallel to the magnetic field inside the electron density cavity along one pair of the separatrices. A low energy electron beam is formed because of this parallel electric field and will flow into the X-line region where electrons are further accelerated by the reconnection electric field [49].

A detailed study of electron acceleration in both anti-parallel reconnection and guide field reconnection was performed by Huang et al. [50] using 2-D full particle simulations. They initially obtained the self-consistent electric field and magnetic field by numerical simulations. Then, by choosing the electric and magnetic fields for some initial times, they studied the electron dynamics of test particles. In this way, the results are unaffected significantly because the characteristic time associated with magnetic reconnection is longer than the characteristic time of the test particles. To understand electron acceleration in detail, different initial positions and energies were considered in the study. In anti-parallel reconnection, electrons initially situated outside of the separatrices are weakly accelerated along the separatrices and obviously by the reconnection electric field around the X-line region, and then stream out along the magnetic field lines. In contrast, electrons initially located inside the separatrices and injected into the X-line region are not obviously accelerated. When entering the pileup region, these electrons are non-adiabatic in nature, because the gyro-radius is comparable to the curvature radius, and are accelerated. Figure 2 shows typical trajectories of electrons crossing the X-point (a) and the pileup region (b) in anti-parallel reconnection. In guide field magnetic reconnection, electrons can be accelerated more easily than in anti-parallel reconnection whereas electrons cannot be accelerated in the pileup region. Independent of the presence or not of a guide field, electrons with relative high energy can be more easily accelerated to higher energy. Figure 3 presents two typical electron trajectories passing through the X-point (a) and the pileup region (b) in the guide field reconnection.

3 Secondary island instability and electron acceleration

Recent simulation results indicate the current sheet in the reconnection diffusion region extends along the outflow directions. Small-scale magnetic islands are created in the expanded current sheet because of secondary island instability

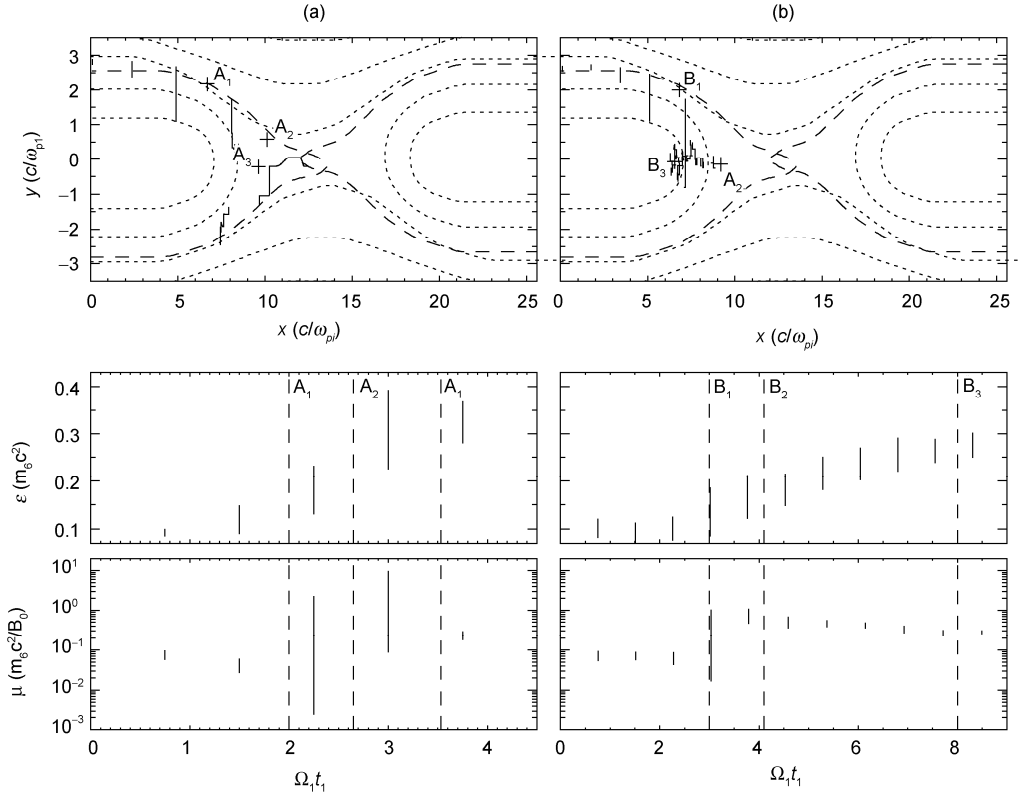

Figure 2 Typical trajectories (top), kinetic energy (middle), and magnetic moment (bottom) of electrons in anti-parallel reconnection. Their initial positions are (a) x=0.1 c/ω_{pi}, y=2.8 c/ω_{pi}, and (b) x=0.1 c/ω_{pi}, y=2.56 c/ω_{pi}. The dashed lines denote magnetic field lines.

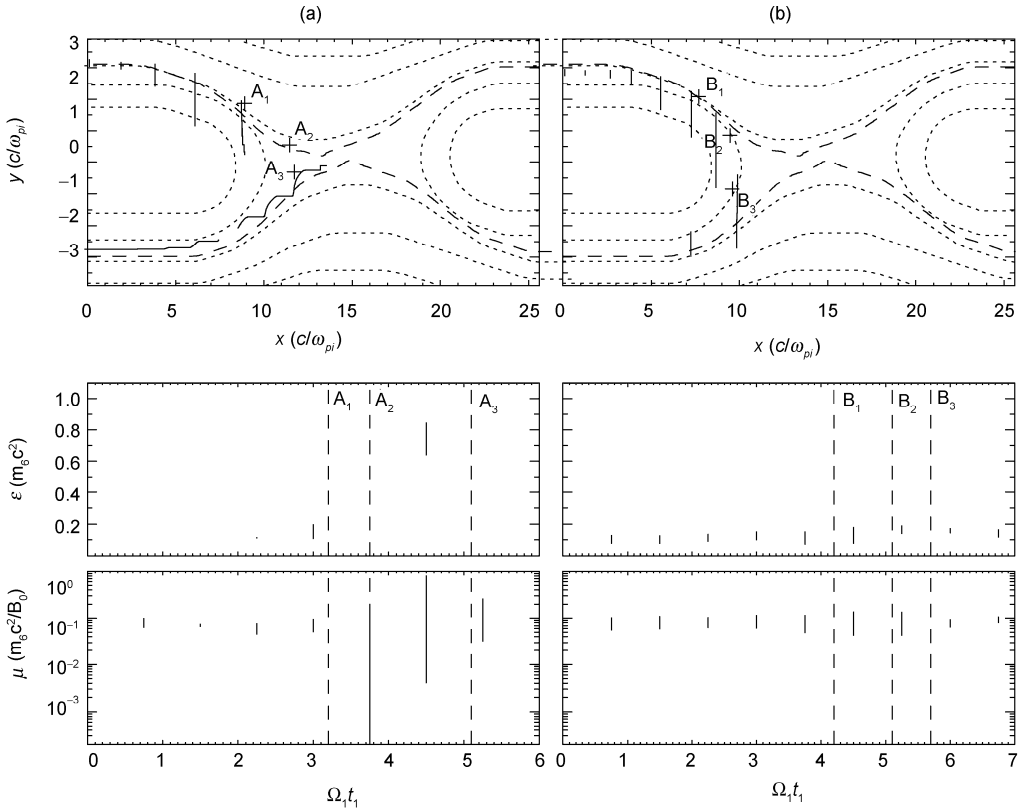

Figure 3 Trajectories (top), kinetic energy (middle), and magnetic moment (bottom) evolutions of two typical electrons in the guide field reconnection. Their initial positions are (a) x=0.1 c/ω_{pi}, y=3 c/ω_{pi} and (b) x=0.1 c/ω_{pi}, y=2.75 c/ω_{pi}. The dashed lines denote magnetic field lines.

[27,51−54]. From full particle simulations, these secondary islands can easily form in guide field magnetic reconnection. In contrast, these fail to form in anti-parallel reconnection because of the short length of the current sheet [51]. Using large scale and open boundaries, Daughton et al. [52] found that in anti-parallel reconnection the current sheet can extend along the outflow directions up to tens of times the ion inertial length. A secondary magnetic island appears in the center of the current sheet because of secondary island instability. This island expands during reconnection and flows out of the diffusion region. As long as secondary islands are continuously created, reconnection will be fast. Furthermore, if the Lundquist number is large enough, the Sweet-Parker reconnection layer will be unstable and a number of islands will be created in the layer [53,54]. While the length of the current sheet between two adjacent magnetic islands is close to the ion inertial length, the reconnection rate will decrease sharply. A continuous increase in the reconnection electric field results in the formation of the electron scale current sheet.

In the Earth's magnetosphere, small-scale magnetic islands, accompanied by high speed flows, have been confirmed several times from spacecraft data. Inside the island, the electric field is very strong and significantly affects particle dynamics [55,56]. Densities and fluxes of energetic electrons peak inside the magnetic islands with electrons displaying isotropic flat-top distributions, as seen in Cluster observations of the magnetotail [57]. Although, the scale of the observed magnetic islands is consistent with predictions from simulations, these islands were all measured in the reconnection outflow region. However, these measurements cannot verify whether these islands were created inside the diffusion region and then jetted out, in the manner for those generated in simulations. Using the Cluster observations of the magnetotail, Wang et al. [45] provided the first evidence that secondary islands can be formed inside the diffusion region as shown in Figure 4. In such events, a squeezed magnetic island with an aspect ratio of 2:1 is detected near the center of the diffusion region. This observation is in accord with predictions of secondary island instabilities in numerical simulations. Moreover, fluxes of energetic electrons increase as the spacecraft traverses the ion diffusion region. Inside the island, the fluxes are further enhanced. Using the current density, electron density, electron pitch angle distribution and waves inside the island, it can be seen that the electron density peaks in the outer region and dips in the core region of the island. Simultaneously, electron beams parallel to the magnetic field lines and currents anti-parallel to such lines are observed in the outer region. Again, the out-of-plane magnetic field arising from the current density is consistent with the observed core magnetic field. According to measurements, an electron beam parallel to the

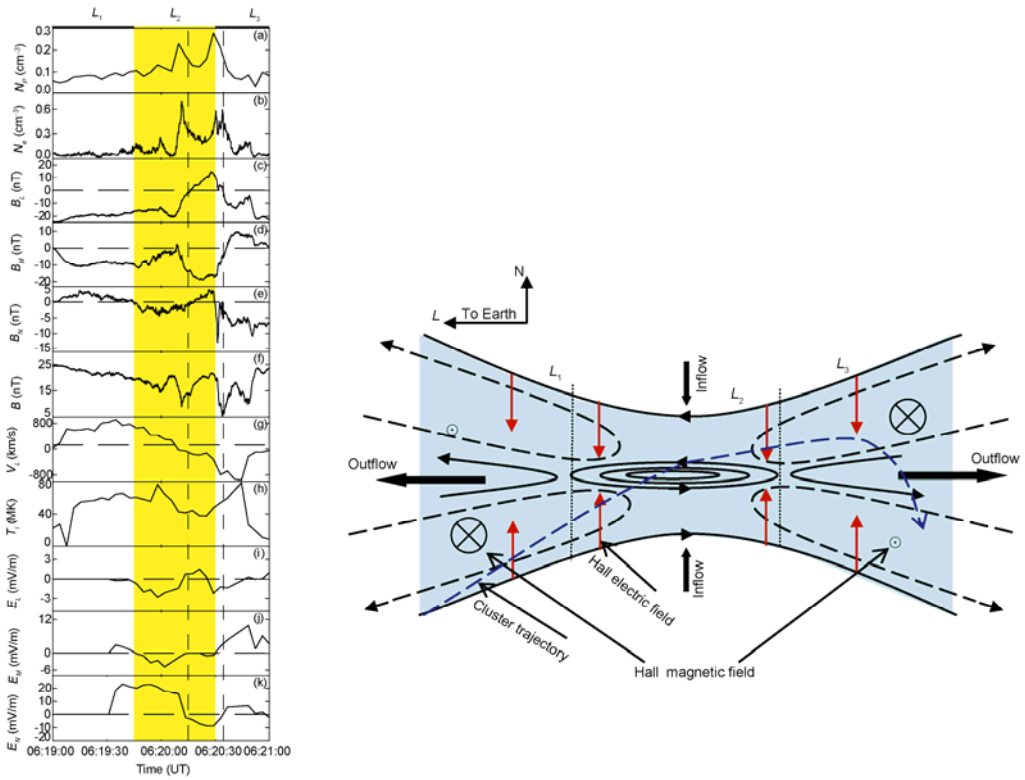

Figure 4 The left panel presents observational data from Cluster's C4 satellite between 06∶19–06∶21 UT on 4 Oct., 2003. From top to bottom, proton density, electron density, the magnetic field vectors B_L, B_M, B_N, the magnitude of the magnetic field B, the L component of the high speed flow, ion temperature and the electric field vectors E_L, E_M, E_N. Subscript N denotes the normal to the current sheet and L points to Earth. L, M and N constitute ta right-handed coordinate system. The right panel illustrates the schematics of the ion diffusion region. The solid lines with arrow are magnetic field lines, the dashed lines represent the Hall current system, and the blue dashed line is the trajectory of Cluster. The red arrows denote the Hall electric field and the circles display the direction of the Hall magnetic field.

magnetic field lines in the outer region forms currents antiparallel to the magnetic field lines, which produces the core magnetic field. Because of the presence of this core magnetic field, electrons will be expelled out of the region and pile up in the outer region, thereby forming the density dip in the core region. Additionally, electron distributions display anisotropy, and fluxes parallel to the magnetic field lines are larger than those perpendicular to these. In the outer region, the distribution is flat-topped, while in the core region the distribution is exponential [58].

4 Magnetic reconnection in laboratory plasmas

Magnetic reconnection can be studied in laboratory experiments. Several laboratory experiments dedicated to magnetic reconnection research have been performed, such as, Large Cathode Device (LCD) and Magnetic Reconnection Experiment (MRX) in the United States, Current Sheet (CS)-3D device in Russia [59].

During investigations of magnetic reconnection without a guide field detected in MRX, Ren et al. [60] encountered using the magnetic probes, the quadrupolar magnetic field structure, thus providing direct evidence of the Hall effect. Changing the electron mean free path, they found that the Hall magnetic field becomes stronger as the process becomes more collisionless. The results indicate that the Hall effect has a key role in collisionless magnetic reconnection. CS-3D device provided indirect evidence of the Hall current in guide field reconnection [61]. They found that in both Ar and Kr plasmas the reconnection current sheet is tilted compared with that in He plasma because of the rotation of J×B from the Hall current due to the guide field.

The experimental evidence for the electron diffusion region was provided by Ren et al. [62] in MRX. They measured the scale of the electron diffusion region and found that the thickness of the region δ_z is about six times the electron inertial length. The maximum of the outflow electron velocity is about one-tenth the Alfvén speed. Moreover, the spatial scale associated with electrons accelerated up to the maximum is unrelated to the electron inertial length, but is about one to two times the ion inertial length. This result is consistent with recent simulations [52]. Furthermore, during magnetic reconnection formed in the plasma produced by the laser, the thickness of the electron diffusion region is also about 10 times the electron inertial length, consistent with the results from MRX [63].

LCD gave direct experimental evidence of electron acceleration during magnetic reconnection [64]. The electron probe curve and emission spectra data indicated that

electrons can be heated and accelerated. Electromagnetic radiation at around the electron plasma frequency was detected, and the radiation is delayed with respect to the peak of the energetic electrons. Such radiation might be produced through enhancement of thermal fluctuations.

Because of the limited range in plasma parameters and spatial resolution, studies on magnetic reconnection in laboratory plasmas are mainly below ion inertial length scales. For electron inertial length scales and smaller, physical processes during reconnection is an unexplored terrain that will be investigated in the near future.

5 Conclusions

Magnetic reconnection provides a physical mechanism for fast energy conversion from magnetic energy to plasma kinetic energy, and is closely associated with many explosive phenomena in space plasma. Electron dynamics is very important for collisionless reconnection. At ion inertial length scales, electron motion determines the current system in the reconnection plane, and simultaneously forms electron density cavities along the separatrices. In anti-parallel reconnection, the in-plane currents stream along the separatrices and are injected into the X-point inside the separatrices. This type of current system forms a symmetric quadrupolar structure with an out-of-plane magnetic field B_y. In the in-plane for guide-field reconnection, current streams out of the X-point along one pair of the separatrices while being injected into the X-point along the magnetic field lines in the inside of the other pair of separatrices. Eventually, B_y is enhanced in the center of the current sheet. Below the electron inertial length scale, anisotropic electron pressure determines the reconnection electric field. In anti-parallel magnetic reconnection, electrons are mainly accelerated by the reconnection electric field at scales below the electron inertial length. In the pileup region, if the gyro-radii are comparable to the curvature radii of the magnetic field, electrons can also be accelerated. However, the efficiency of electron acceleration and the role of acceleration in the pileup region are still a questionable issues. In guide field reconnection, electrons flowing into the X-point along the separatrices can be accelerated by the parallel electric field, and further accelerated in the electron inertial region. It is still not very clear how at scales below the electron inertial length the anisotropic distribution of electron pressure is formed and what the relationship between the distribution and energetic electrons is.

Nevertheless, acceleration is limited because electrons cannot be trapped effectively at a single X-point. Recent observations and theoretical research indicate that secondary islands can be formed around the X-point. Secondary islands not only may raise the reconnection rate but also trap electrons within the region carrying a reconnection electric field. Thus, electrons can be accelerated with more efficiency. However, how electrons are accelerated in the secondary island is still an open question. Additionally, waves are enhanced in reconnection; both lower hybrid waves and whistler waves are observed. The relationship between waves and electron acceleration is also an unresolved problem [65,66].

In brief, although great progress on the relationship between electron dynamics and collisionless magnetic reconnection has been made, a great number of issues still remain open and more studies are needed.

This work was supported by the National Natural Science Foundation of China (40725013, 40974081 and 40931053), the Chinese Academy of Sciences (KJCX2-YW-N28) and the Ocean Public Welfare Scientific Research Project, State Oceanic Administration of China (201005017).

1 Wang S, Lee L. Magnetic Reconnection (in Chinese). Hefei: Anhui Educational Press, 1999
2 Biskamp D, Magnetic Reconnection in Plasma. Cambridge: Cambridge University Press, 2000
3 Priest E, Forbes T. Magnetic Reconnection: MHD Theory and Applications. Cambridge: Cambridge University Press, 2000
4 Tsuneta S, Hara H, Shimizu T, et al. Observation of a solar flare at the limb with the Yohkoh Soft X-ray Telescope. Publ Astron Soc Jpn, 1992, 44: L63–L69
5 Cargill P A, Klimchuk J A. A nanoflare explanation for the heating of coronal loops observed by Yohkoh. Astrophys J, 1997, 478: 799
6 Nishida A. Geomagnetic Diagnostics of the Magnetosphere. New York: Springer, 1978
7 Ge Y S, Russell C T. Polar survey of magnetic field in near tail: Reconnection rare inside 9 R_E. Geophys Res Lett, 2006, 33: L02101
8 Wesson J. Tokomaks. New York: Oxford University Press, 1997
9 Giovanelli R G. A theory of chromospheric flares. Nature, 1946, 158: 81–82
10 Dungey J W. Cosmic Electrodynamics. New York: Cambridge University Press, 1958
11 Sweet P A. The neutral point theory of solar flares. In: Lehnert B, ed. Electro-magnetic Phenomena in Cosmical Physics. New York: Cambridge University Press, 1958
12 Parker E N. Sweet's mechanism for merging magnetic fields in conducting fluids. J Geophys Res, 1957, 62: 509–518
13 Petschek H G. Magnetic annihilation. In: Hess W N, ed. AAS-NASA Symposium on the Physics of Solar Flares, NASA Spec PublSp-50, 1964
14 Birn J, Drake J F, Shay M A, et al. Geospace Environmental Modeling (GEM) magnetic reconnection challenge. J Geophys Res, 2001, 106: 3715–3720
15 Sonnerup B U Ö. Magnetic field reconnection. In: Lanzèerotti L J, Kennel C F, Parker E N, eds. Solar System Plasma Physics. 1979, 310: 46
16 Shay M A, Drake J F, Rogers B N, et al. Alfvénic collisionless magnetic reconnection and the Hall term. J Geophy Res, 2001, 106: 3759–3772
17 Ma Z W, Bhattacharjee B. Hall magnetohydrodynamic reconnection: The geospace environment modeling challenge. J Geophys Res, 2001, 106: 3773–3782
18 Pritchett P L. Geospace Environment Modeling magnetic reconnection challenge: Simulations with a full particle electromagnetic code. J Geophys Res, 2001, 106: 3783–3798
19 Rogers B N, Denton R E, Drake J F. Signatures of collisionless magnetic reconnection. J Geophys Res, 2003, 108: 1111–1117
20 Huang C, Wang R, Lu Q, et al. Electron density hole and quadruple structure of B_y during collisionless magnetic reconnection. Chinese Sci Bull, 2009, 54: 3852–3857

21 Wang R S, Lu Q M, Huang C, et al. Multi-spacecraft observation of electron pitch angle distributions in magnetotail reconnection. J Geophys Res, 2010, 115: A01209
22 Øieroset M, Phan T D, Fujimoto M, et al. *In situ* detection of collisionless reconnection in the Earth's magnetotail. Nature, 2001, 412: 414–417
23 Nagai T, Shinohara I, Fujimoto M, et al. Geotail observations of the Hall current system: Evidence of magnetic reconnection in the magnetotail. J Geophys Res, 2001, 106: 25929
24 Nagai T, Shinohara I, Fujimoto M, et al. Structure of the Hall current system in the vicinity of the magnetic reconnection site. J Geophys Res, 2003, 108: 1357–1364
25 Fu X R, Lu Q M, Wang S. The process of electron acceleration during collisionless magnetic reconnection. Phys Plasmas, 2006, 13: 012309
26 Hesse M, Winske D. Electron dissipation in collisionless magnetic reconnection. J Geophys Res, 1998, 103: 26479
27 Hesse M, Schindler K, Birn J, et al. The diffusion region in collisionless magnetic reconnection. Phys Plasmas, 1999, 6: 1781
28 Kuznetsova M, Hesse M, Winske D. Collisionless reconnection supported by non-gyrotropic pressure effects in hybrid and particle simulations. J Geophys Res, 106: 3799
29 Hesse M, Kuznetsova M, Hoshino M. The structure of the dissipation region for component reconnection: Particle simulations. Geophys Res Lett, 2002, 29: 1563
30 Guo J, Lu Q M. Effects of ion-to-electron mass ratio on electron dynamics in collisionless magnetic reconnection. Chin Phys Lett, 2007, 24: 3199
31 Wan W G, Lapenta G. Electron self-reinforcing process of magnetic reconnection. Phys Rev Lett, 2008, 101: 015001
32 Lu Q M, Huang C, Xie J L, et al. Features of separatrix regions in magnetic reconnection: Comparison of 2D particle-in-cell simulations and Cluster observations. J Geophys Res, 2010, 115: A11208
33 Fujimoto M, Nakamura M S, Shinohara I, et al. Observations of earthward streaming electrons at the trailing boundary of a plasmoid. Geophys Res Lett, 1997, 24: 2893–2896
34 Manapat M, Øieroset M, Phan T D, et al. Field-aligned electrons at the lobe/plasma sheet boundary in the mid-to-distant magnetotail and their association with reconnection. Geophys Res Lett, 2006, 33: L05101
35 Retino A, Vaivads A, Andre M, et al. Structure of the separatrix region close to a magnetic reconnection X-line: Cluster observations. Geophys Res Lett, 2006, 33: L06101
36 Retino A, Nakamura R, Vaivads A, et al. Cluster observations of energetic electrons and electromagnetic fields with a reconnecting thin current sheet in the Earth's magnetotail. J Geophys Res, 2008, 113: A12215
37 Mozer F S, Bale S D, Phan T D. Evidence of diffusion regions at a subsolar magnetopause crossing. Phys Rev Lett, 2002, 89: 015002
38 Vaivads A, Khotyaintsevy Y V, Andre M, et al. Structure of the magnetic reconnection diffusion region from four-spacecraft observations. Phys Rev Lett, 2004, 93: 105001
39 Khotyaintsev Y V, Vaivads A, Retino A, et al. Formation of inner structure of a reconnection separatrix region. Phys Rev Lett, 2006, 97: 205003
40 Pritchett P L, Coroniti F V. Three-dimensional collisionless magnetic reconnection in the presence of a guide field. J Geophys Res, 2004, 109: A01220
41 Lu S, Lu Q M, Huang C, et al. The effects of the guide field on the structures of electron density depletions in collisionless magnetic reconnection. Chinese Sci Bull, 2011, 1: 48–52
42 Vasyliunas V M. Theoretical models of magnetic field line merging. J Geophys Res, 1975, 13: 303–336
43 Øieroset M, Lin R P, Phan T D, et al. Evidence for electron acceleration up to ~300 keV in the magnetic reconnection diffusion region of Earth's magnetotail. Phys Rev Lett, 2002, 89: 195001
44 Wang R S, Lu Q M, Guo J, et al. Spatial distribution of energetic electrons during magnetic reconnection. Chin Phys Lett, 2008, 25: 3083
45 Wang R S, Lu Q M, Du A M, et al. *In situ* observations of a secondary magnetic island in an ion diffusion region and associated energetic electrons. Phys Rev Lett, 2010, 104: 175003
46 Hoshino M, Mukai T, Terasawa T, et al. Suprathermal electron acceleration in magnetic reconnection. J Geophys Res, 2001, 106: 25979
47 Pritchett P L. Relativistic electron production during driven magnetic reconnection. Geophys Res Lett, 2006, 33: L13104
48 Guo J, Lu Q M, Wang S, et al. Electron acceleration in collisionless magnetic reconnection. Chin Phys Lett, 2005, 22: 409
49 Pritchett P L. Relativistic electron production during guide field magnetic reconnection. J Geophys Res, 2006, 111: A10212
50 Huang C, Lu Q M, Wang S. The mechanisms of electron acceleration in anti-parallel and guide field magnetic reconnection. Phys Plasmas, 2010, 17: 072306
51 Drake J F, Swisdak M, Schoeffler M, et al. Formation of secondary islands during magnetic reconnection. Geophys Res Lett, 2006, 33: L13105
52 Daughton W, Scudder J, Karimabadi H. Fully kinetic simulations of undriven magnetic reconnection with open boundary conditions. Phys Plasma, 2006, 13: 072101
53 Daughton W, Roytershteyn V, Albright B J, et al. Transition from collisional to kinetic regimes in large-scale reconnection layers. Phys Rev Lett, 2009, 103: 065004
54 Samtaney R, Loureiro N F, Uzdensky D A, et al. Formation of plasmoid chains in magnetic reconnection. Phys Rev Lett, 2009, 103: 105004
55 Eastwood J P, Phan T D, Mozer F S, et al. Multi-point observations of the Hall electromagnetic field and secondary island formation during magnetic reconnection. J Geophys Res, 2007, 112: A06235
56 Chen L J, Bhattacharjee A, Puhl-Quinn P A, et al. Observation of energetic electrons within magnetic islands. Nature Phys, 2008, 4: 19–23
57 Chen L J, Bessho N, Lefebvre B, et al. Multi-spacecraft observations of the electron current sheet, neighboring magnetic islands, and electron acceleration during magnetotail reconnection. Phys Plasmas, 2009, 16: 056501
58 Wang R S, Lu Q M, Li X, et al. Observations of energetic electrons up to 200 keV associated with a secondary island near the center of an ion diffusion region: A Cluster case study. J Geophys Res, 2010, 115: A11201
59 Yamada M, Kulsrud R, Ji H. Magnetic reconnection. Rev Modern Phys, 2010, 82: 603–664
60 Ren Y, Yamada M, Gerhardt S, et al. Experimental verification of the Hall Effect during magnetic reconnection in a laboratory plasma. Phys Rev Lett, 2005, 95: 055003
61 Frank A G, Bogdanov S Yu, Dreiden G V, et al. Structure of the current sheet plasma in the magnetic field with an X line as evidence of the two-fluid plasma properties. Phys Lett A, 2006, 348: 318–325
62 Ren Y, Yamada M, Ji H, et al. Identification of the electron-diffusion region during magnetic reconnection in a laboratory plasma. Phys Rev Lett, 2008, 101: 085003
63 Zhong J Y, Li Y T, Wang X G, et al. Modelling loop-top X-ray source and reconnection outflows in solar flares with intense lasers. Nature Phys, 2010, 6: 984–987
64 Stenzel R L, Urrutia J M, Griskey M, et al. A new laboratory experiment on magnetic reconnection. Phys Plasmas, 2002, 9: 1925
65 Wei X H, Cao J B, Zhou G C, et al. Cluster observations of waves in the whistler frequency range associated with magnetic reconnection in the Earth's magnetotail. J Geophys Res, 2007, 112: A10225
66 Guo F, Lu Q M, Guo J, et al. Nonlinear evolution of lower hybrid drift instability in Harris Current. Chin Phys Lett, 2008, 25: 2725–2728